

An Efficient *a Posteriori* Treatment for Dispersion Interaction in Density-Functional-Based Tight Binding

Lyuben Zhechkov,[†] Thomas Heine,^{*,†} Serguei Patchkovskii,[‡] Gotthard Seifert,[†] and Helio A. Duarte[§]

Institut für Physikalische Chemie und Elektrochemie, TU Dresden, D-01062 Dresden, Germany, Steacie Institute for Molecular Sciences, NRC, 100 Sussex Dr., Ottawa, Ontario K1A 0R6, Canada, and Departamento de Química-ICEx, Universidade Federal de Minas Gerais, 31270-901 Belo Horizonte, Brazil

Received March 14, 2005

Abstract: The performance of density functional theory (DFT) (VWN-LDA, PBE-GGA, and B3LYP hybrid functionals), density-functional-based tight binding (DFTB), and ab initio methods [HF, MP2, CCSD, and CCSD(T)] for the treatment of London dispersion is investigated. Although highly correlated ab initio methods are capable of describing this phenomenon, if they are used with rather large basis sets, DFT methods are found to be inadequate for the description of H₂/PAH (polycyclic aromatic hydrocarbon) interactions. As an alternative approach, an *a posteriori* addition of a van der Waals term to DFTB is proposed. This method provides results for H₂/PAH interactions in close agreement with MP2 and higher-level ab initio methods. Bulk properties of graphite also compare well with the experimental data.

1. Introduction

One of the weakest, qualitatively important interactions between molecules, fragments of molecules, solutes, and solids is the dispersion interaction, named after F. London, who gave the first physical description of this phenomenon. In his famous formula,¹ dispersion is described as the interaction of two neutral, separated particles with a non-overlapping charge density and without a permanent dipole moment. The dispersion energy depends on the distance between the particles r , the polarizabilities α'_1 and α'_2 , and the ionization energies of the interacting particles I_1 and I_2 : Hence, dispersion between nonpolar molecules is always

$$U_{\text{London}} = -\frac{2}{3} \frac{I_1 I_2}{I_1 + I_2} \alpha'_1 \alpha'_2 \frac{1}{r^6} \quad (1)$$

attractive and slowly falls off as r^{-6} . It is several orders of

magnitude weaker than typical covalent or ionic interactions and still a factor of 10 smaller than hydrogen bridge bonds. Despite this simple physical picture, a straightforward *first principle* quantum-mechanical description of the interaction is not trivial.

Density functional theory (DFT) within the Kohn–Sham formulation and with presently available exchange-correlation functionals does not describe the dispersion interaction correctly.² Within the local density approximation (LDA), the inherent overbinding of the method leads to a strong overestimation of the interaction around the van der Waals minimum and does not provide the correct long-range behavior.^{2–4} On the other hand, GGA DFT is able to reproduce the order of magnitude of the dispersion interaction close to the van der Waals minimum.⁵ At the same time, it also fails to handle the long-range part of the potential and is, hence, not appropriate, for instance, in the simulation of physisorption processes.⁴ The true correlation energy functional must include the van der Waals interaction,⁶ and future generations of optimized effective potentials^{2,7–10} may correct this deficiency of DFT. Indeed, considerable progress has been achieved toward a better description of weak interactions within DFT by the TPSS family of meta-GGAs, which

* Corresponding author e-mail: thomas.heine@chemie.tu-dresden.de.

[†] Institut für Physikalische Chemie und Elektrochemie, TU Dresden.

[‡] Steacie Institute for Molecular Sciences, NRC.

[§] Universidade Federal de Minas Gerais.

improve results, in particular, for the short range.^{11,12} Direct inclusion of London forces into the nonlocal part of the correlation potential¹³ and into pseudopotentials¹⁴ has been suggested recently. An a posteriori correction to the BLYP functional has been proposed by Grimme.⁷ His method focuses on the correction of the long-range part of the interaction by employing a C_6 term, while the interaction is switched off by an expression that has been tuned for the PBE and the BLYP functionals. However, at present, only post-Hartree–Fock (HF) ab initio computations with a reasonable description of correlation {for example, second-order Møller–Plesset perturbation theory (MP2), or coupled cluster theory including single, double (CCSD), and (partially) triple excitations [CCSD(T)]} are capable of treating this interaction properly for the short and, in particular, the long distance. Unfortunately, such calculations require nearly converged basis sets and, therefore, a high computational effort.^{15,16} On the other hand, the density-functional-based tight-binding (DFTB) methods with and without self-consistent charge (SCC) correction^{17–19} are known to completely exclude van der Waals interactions, and a correction by the a posteriori addition of a C_6 term has been proposed for DFTB.²⁰ For an overview of the DFTB method and its applications, see ref 21.

A working methodology that includes the dispersion interaction is a necessity, as many fundamental processes in chemistry, physics, and biology are strongly affected by this weak long-range interaction, for example, the geometry of molecular crystals, the structure of biological molecules, surface–adsorbate interactions, π – π stacking interactions, and so forth. In contrast to other long-range interactions, such as the Coulomb interaction of charged particles, the van der Waals interaction between two nonpolar particles is always attractive. Although the van der Waals term falls off as r^{-6} with the distance r , in the region of up to ~ 6 Å, its contributions to the interparticle interactions is still not negligible. Although the dispersion interaction influences the long-range interaction energy, its short-range effect on covalent bond parameters and on certain electronic properties can be neglected—van der Waals type interactions are orders of magnitude smaller than covalent bonds.^{15,16,22,23} Several methods take advantage of this fact and treat long-range interaction by adding a van der Waals term to energies and gradients.^{20,24} This strategy is easy to follow for the attractive, long-range part of the potential energy surface (PES). Indeed, in this part of the PES, the dispersion or the general van der Waals interaction is clearly dominating part of the correlation energy and may be described independently from all other contributions.

At shorter distances, the interaction energy is dominated by electronic overlap effects. The a posteriori term should have no influence on those interatomic distances that are characteristic for covalent bonds. Several techniques have been introduced to avoid problems with the short-range part of an a posteriori-added van der Waals potential: In Rappé’s universal force field (UFF),²⁴ the van der Waals contribution is only considered for interatomic interactions where the two atoms are not adjacent to each other or to a common neighbor. Other implementations use a switching function

to turn off the van der Waals potential at short distances or employ lists of “van der Waals-active” interatomic contacts.²⁰

The aim of this work is to provide a quantum-chemical method that is extended with a parameterized van der Waals potential in such a way that no contact lists need to be employed and that the van der Waals parameters are available throughout the periodic table. As our main target application is to describe carbon nanostructures, we have chosen the DFTB method as a quantum-mechanical basis, as it clearly excludes van der Waals interaction and is capable of simulating large structures. This aim is achieved by switching between two different analytical descriptions for the van der Waals term for the short- and long-range parts. Our implementation takes advantage of available Lennard–Jones parameters of the UFF force field,²⁴ which are optimized to reproduce van der Waals distance, well depth, and local curvature and which are available from H to Lw.²⁴

In the first part of this article, we compare the performance of DFTB, ab initio, and DFT methods for the dispersion interaction of H_2 with PAHs. Then, we describe augmentation of the DFTB method with a dispersion term and its implementation in the deMon code.²⁵

Finally, we evaluate the performance of the new technique for the interaction of H_2 with PAHs and for the structural and elastic properties of graphite.

II. Benchmark Calculations

A. Geometries and Computational Methodology. The interaction of H_2 with some PAHs has been studied previously, and we take all PAH geometries from previous work.¹⁵ The PAH structures have been optimized at the B3LYP/6-31G* level, previously shown to give geometries very close to those of MP2 computations.¹⁵ The basis set superposition errors (BSSE) have been corrected by applying the counterpoise methodology.²⁶ All DFT- and DFTB-based computations except those with hybrid functionals have been performed using deMon.²⁵ MP2 calculations and DFT with hybrid functionals have been carried out using Gaussian 03 software,²⁷ whereas CCSD and CCSD(T) energies were obtained using NWChem.²⁸

B. Ab Initio Methods. In Figure 1 and Table 1, a series of ab initio computations on H_2 motion along the normal to benzene plane are compared, including MP2 with several basis sets with and without correcting for BSSE and two coupled cluster approaches (with and without the perturbative triples correction). Strong dependence of the MP2 results with respect to the orbital basis shows the importance of the basis set convergence. Thus, only with large augmented basis sets does MP2 approach a converged result. For the largest basis set studied, aug-cc-pVQZ,²⁹ the BSSE is smaller than 1 kJ mol⁻¹.¹⁵ On the other hand, MP2 calculations of H_2 /benzene¹⁵ and N_2 /benzene²² for various distances and orientations of the physisorbed molecule with respect to benzene showed that the cc-pVTZ basis, without correcting for BSSE, gives very similar results to those of BSSE-corrected MP2/aug-cc-pVQZ interaction energies for a large range of interatomic distances (see Figure 1). Employing the cc-pVTZ basis, the level of correlation has been increased in coupled cluster calculations with single and double

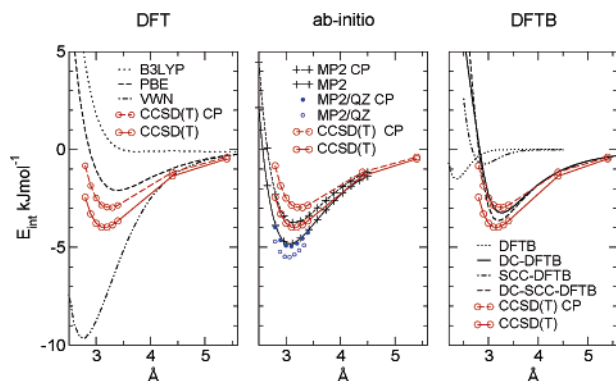


Figure 1. Potential energy surface for H_2 motion along the C_6 axis normal to benzene plane at various levels of ab initio and DF theory, with and without counterpoise (CP) corrections for the BSSE, and dispersion-corrected (DC) and uncorrected DFTB and SCC DFTB. All ab initio and DFT calculations employed the cc-pVTZ basis set, except for QZ, which denotes the aug-cc-pVQZ basis set. Results for other basis sets are given in Table 1.

Table 1. Interaction Energies of H_2 with Benzene^a

method	R_{int}	E_{int}
VWN/DZVP	2.8(2.8)	-8.77(-8.22)
VWN/TZVP	2.8(2.8)	-9.34(-8.69)
VWN/cc-pVTZ	2.8(2.8)	-9.62(-9.28)
PBE/DZVP	3.4(3.4)	-2.08(-1.62)
PBE/TZVP	3.4(3.5)	-2.12(-1.70)
PBE/cc-pVTZ	3.4(3.4)	-2.10(-1.90)
B3LYP/DZVP	3.7(3.7)	-0.04(+0.25)
B3LYP/TZVP	3.7(3.7)	-0.17(+0.10)
B3LYP/cc-pVTZ	3.7(3.7)	-0.11(+0.04)
HF/cc-pVTZ	4.0(4.0)	-0.55(-0.48)
MP2/6-31G*	3.7(3.4)	-2.56(-0.96)
MP2/6-311G**	3.2(3.4)	-4.16(-2.07)
MP2/pVTZ	3.1(3.4)	-3.78(-2.16)
MP2/cc-pVTZ	3.1(3.2)	-4.82(-3.74)
MP2/aug-cc-pVTZ	3.0(3.1)	-6.64(-4.72)
MP2/aug-cc-pVQZ	3.0(3.1)	-5.51(-4.94)
CCSD/cc-pVTZ	3.2(3.3)	-3.33(-2.53)
CCSD(T)/cc-pVTZ	3.2(3.3)	-3.97(-2.97)
DFTB	2.4	-1.51
DC DFTB	3.3	-3.25
SCC DFTB	2.9	-0.75
DC SCC DFTB	3.2	-3.64

^a Interaction energies are given in kJ mol^{-1} and equilibrium distances in \AA . Numbers in parentheses include counterpoise corrections for BSSE.

excitations (CCSD) and perturbation of triple excitations [CCSD(T)]. For the final estimation of the H_2 /benzene interaction, we used the best level of correlation treatment of our computations [CCSD(T)], employing a cc-pVTZ basis, because, for the H_2 /benzene system, interaction energies calculated with this basis nearly coincide with the extrapolation of the basis set limit. We found the interaction energy slightly reduced (by $\sim 0.8 \text{ kJ mol}^{-1}$ with respect to MP2/cc-pVTZ), and the overall interaction in Figure 1 shows the same trend as that for MP2. With these results, we estimate the H_2 /benzene interaction energy to be $4.2\text{--}4.7 \text{ kJ mol}^{-1}$ and the intermolecular equilibrium distance to be $3.1\text{--}3.3 \text{ \AA}$.

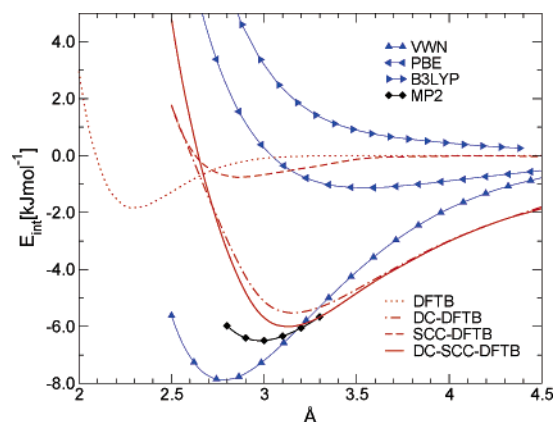


Figure 2. Potential energy surface of H_2 motion normal to the center of coronene. Details and conventions are the same as those in Figure 1.

C. Density Functional Theory. Even though the unknown exact correlation energy functional must include dispersion,⁶ all present popular functionals fail to describe this type of interaction for some parts of the potential energy surface.² Figures 1 and 2 illustrate the performance of three representative DFT methods with a double- ζ (DZVP³⁰) and two different triple- ζ basis sets including polarization functions (TZVP³⁰ and cc-pVTZ³¹). The three types of functionals are the LDA proposed by Vosko, Wilk, and Nusair (VWN);³² a recent highly respected GGA (PBE);³³ and the B3LYP hybrid functional.^{34,35} In all three functionals, the performance is independent of the employed basis set, and they have only small BSSEs, as can be seen in Table 1. For the H_2 /benzene complex (Figure 1), LDA overestimates the attraction by a factor of more than 2 and finds the equilibrium distance at 2.8 \AA —approximately 0.3 \AA shorter than more elaborate theories. On the other hand, PBE slightly underestimates the interaction and finds the van der Waals minimum at distance 3.4 \AA , too long by about 0.3 \AA , so this method performs rather well for H_2 /benzene. The admixture of the exact HF exchange in the B3LYP functional is clearly not beneficial for treatment of dispersion interactions. When considering coronene, a larger PAH, the failure of popular DFT methods to describe the dispersion interaction is even more evident (see Figure 2). All three DFT variants examined here, including the PBE functional, not only fail to give a reasonable description of the long-range potential but even find the interaction of H_2 with coronene less attractive than with benzene—opposite of the ab initio results and physical expectations based on eq 1. In summary, modern GGAs can give equilibrium distances of van der Waals complexes to good accuracy, a conclusion that is supported by our PBE calculations and by more extensive studies employing the somewhat similar PW91 functional.^{5,15} The three functionals compared in this study are unsuitable for the study of large van der Waals complexes, as they show unphysical trends for adsorption energy when comparing PAHs of different size and incorrect long-range behavior.

D. DFTB and its van der Waals Extension. DFTB can be considered as an approximation to DFT.^{17–19} It treats short-range atomic potentials and neglects three-center terms in the Hamiltonian. Hamilton matrix elements fall off quickly

and become negligible for interatomic distances typical for the region of the van der Waals minimum. Hence, dispersion is not included in the DFTB electronic Hamiltonian. In both available parameterizations (non-SCC¹⁸ and SCC¹⁹), DFTB shows only a very small attractive potential at distances shorter than the van der Waals minimum (see Figures 1 and 2). Therefore, the addition of an empirical van der Waals correction does not introduce artificial “double counting” of dispersion in the vicinity of the van der Waals minimum, as it could for DFT computations that already include some dispersion. For practical reasons, we decided to use the parameterization of UFF for the dispersion correction.²⁴ The dispersion interaction U_{ij} between atoms i and j at distance r is given in Lennard–Jones-type form, which includes two parameters: van der Waals distance (r_{ij}) and well depth (d_{ij}). These UFF parameters are reported in the original paper²⁴

$$U_{ij}(r) = d_{ij} \left[-2 \left(\frac{r_{ij}}{r} \right)^6 + \left(\frac{r_{ij}}{r} \right)^{12} \right] \quad (2)$$

and are available throughout the periodic table. In UFF, the van der Waals term is set to zero for those interatomic interactions where the atoms are adjacent either to each other or to a common neighbor atom. Interaction cutoffs based on adjacency information postulate an inflexible topology of the system during the whole simulation and would impose unnecessary restrictions to a quantum-mechanical method. Therefore, a different technique to change the asymptotic behavior for short distances in the analytic form of eq 2 is necessary. As can be inferred from Figures 1 and 2, the additional van der Waals term must include the long-range part and the area around the van der Waals distance to provide a reasonable description of the dispersion interaction. However, the empirical r^{-12} repulsive term conflicts with the quantum-mechanical description for particles with overlapping charge densities, and application of eq 2 for short interatomic distances remains useless. Instead, the van der Waals correction at small interatomic distances should converge to a finite limit. We have chosen to use the Lennard–Jones representation of eq 2 for the whole range of r where U_{ij} is attractive. For a shorter range of r , U_{ij} becomes repulsive. This appears, at first glance, to be surprising, but the necessity to have a repulsive, short-range term is obvious when looking at Figures 1 and 2; the Pauli repulsion between two molecules does not yet appear in DFTB and SCC DFTB for distances at the van der Waals minimum, or even at $r_0 = 2^{-1/6}r_{ij}$, the value at which the Lennard–Jones energy is zero ($U_{ij} = 0$). To maintain numerical stability, we continue the description of the additional potential for distances smaller than r_0 by a polynomial.

$$U_{ij}^{(\text{short-range})}(r) = U_0 - U_1 r^n - U_2 r^{2n} \quad (3)$$

The parameters U_0 , U_1 , and U_2 are determined such that the interaction energy and its first and second derivatives match those of eq 2 at r_0 . In this way, we maintain continuity for energies, forces, and Hessians. Tests for various systems, including the test cases, a series of DNA–carbon-nanotube interactions, water clusters, and cyclodextrine in water—

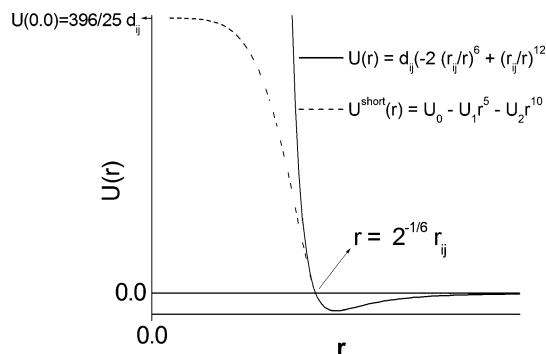


Figure 3. Potential for the dispersion correction to DFTB: The long-range contribution (solid line) is identical for the van der Waals parametrization of UFF (eq 2) up to the point where $U(r) = 0$. The short-range interaction (dashed line) is given by eq 3.

which will be published separately—suggested $n = 5$ as an appropriate choice for the short-range parametrization. For $n = 5$, the parameters U_0 , U_1 , and U_2 of eq 2 are given by Note that d_{ij} is positive in eqs 4–6. The repulsion of our

$$U_0 = \frac{396}{25} d_{ij} \quad (4)$$

$$U_1 = 2^{5/6} \frac{672}{25} \frac{d_{ij}}{r_{ij}^5} \quad (5)$$

$$U_2 = -2^{2/3} \frac{552}{25} \frac{d_{ij}}{r_{ij}^{10}} \quad (6)$$

van der Waals correction is limited by the value of $U_0 \approx 16d_{ij}$ (see Figure 3), a value that is small compared to typical covalent bond energies. Figures 1 and 2 show the performance of dispersion-corrected (DC) and uncorrected DFTB with and without SCC correction compared to our best ab initio reference computations. The agreement of the parameterization and ab initio computations is remarkably good, so that reparameterization of the UFF van der Waals parameters is not necessary, at least for the presently studied systems. The short-range interaction is slightly too repulsive but is dominated in the covalent area by the quantum part of the potential and, hence, is unproblematic. The interaction energy of 3–3.5 kJ mol⁻¹ for H₂/benzene is close to the CCSD(T) value, and the equilibrium distance is found to be slightly overestimated by 0.1 Å. More importantly, the long-range part of the potential is described correctly.

The DFTB method is known as a fast quantum-chemical computational tool. It produces good results for various kinds of carbon-based systems.^{18,36,37} For such systems, we now propose to use the dispersion-corrected variant, allowing extension to systems with non-negligible dispersion interactions. We have implemented this as an extension in the experimental version of the deMon computer code.²⁵

III. Test Applications

A. H₂/PAH and H₂/Graphene Interactions. The DC methodology is applied to a series of H₂/PAH complexes. The MP2 physisorption energies for benzene, naphthalene, anthracene, coronene, and triphenylene have been reported

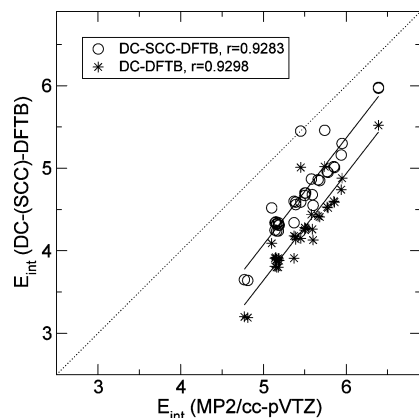


Figure 4. Correlation between MP2 and DC DFTB. SCC DFTB results are given as circles, and DFTB results are given as asterisks. All values are in kJ mol^{-1} . r denotes the correlation coefficient.

in an earlier paper¹⁵ and are used to benchmark our new method. One of the key observations of our earlier work was that the interaction energies of such complexes can easily be obtained with single-point calculations for a system where H_2 is coordinated to the ring center, perpendicular to the molecular plane, with an intermolecular distance of ~ 3.2 Å between the centers of H_2 and the ring. The good performance of the empirical correction is evident when it is compared with the ab initio results in a scatter plot, as shown in Figure 4.

A real advantage of the DC DFTB approach is the possibility to optimize the geometry of such complexes at a low computational cost. Full geometry optimization of the whole set of H_2/PAH complexes shows that all structures correspond to local minima. In general, the DC SCC DFTB bond lengths are found to be slightly longer compared with MP2 computations (≈ 0.02 Å for C–C bonds, ≈ 0.05 Å for H–H bonds, and ≈ 0.1 Å for intermolecular distances). Nevertheless, in the fully optimized structures, the H_2 molecules are slightly tilted, pointing from the ring centers away from the molecule, if they are not physisorbed at the central ring of the PAH. Such trends have been previously reported for $\text{H}_2/\text{C}_6\text{H}_5\text{X}$ ($\text{X} = -\text{F}, -\text{OH}, -\text{CN}, -\text{NH}_2$) systems using coupled cluster theory.¹⁶ For the fully optimized structures, the DC DFTB schemes give interaction energies slightly lower than those of MP2/cc-pVTZ, which is, at least for the studied $\text{H}_2/\text{benzene}$ complex, an excellent result, as it matches our highest-level computation at the CCSD(T) level within 0.5 kJ mol^{-1} (see Figure 1).

Since the dispersion interaction of H_2 with PAHs increases with the PAH size, the upper limit for this interaction is expected for the infinite graphene sheet.¹⁵ To test the present methodology, the interaction energy per molecule between a single graphene layer and H_2 molecules, covering it in such way that at least one empty hexagon lies between two H_2 adsorption sites, has been calculated. The calculations have been carried out using periodic boundary conditions applied for super cells containing 196 carbon atoms. The calculated dispersion energy per H_2 is found to be 6.75 kJ mol^{-1} for DFTB and 7.03 kJ mol^{-1} for SCC DFTB. This result is in

excellent agreement with our previous estimate of 7.6 kJ mol^{-1} , based on MP2/cc-pVTZ calculations.¹⁵

B. Bulk Properties of Graphite. The van der Waals interaction plays a crucial role for the bulk properties of graphite. If the graphite interlayer interaction is described properly, the method may be recommended for applications in the popular area of nanostructures, allowing the study of multiwalled nanotubes, nano-onions, nanotube junctions, peapods, DNA stacking, and so forth. To derive the equilibrium lattice parameters of a single graphene layer, we computed the cohesive energy (see Figure 5) applying periodic boundary conditions on a hexagonal graphene sheet containing 140 atoms. Large super cells are required to justify the Γ -point approximation. We found the value of 2.465 Å for the lattice parameter a , which is in excellent agreement with the X-ray experiment, which yields a value of 2.462 Å,³⁸ and corresponds to a C–C distance of 1.421 Å. As a result of the repulsive character of our correction for short-range diatomic interactions, the cohesive energy of -9.01 eV per atom is slightly lower than the reported -9.24 eV per atom for the same method without van der Waals correction.¹⁸ The equilibrium interlayer distance has been calculated in a super cell containing 560 atoms, that is, with 140 atoms per layer and four layers in an ABABAB arrangement, also known as Bernal graphite. The dependence of the interaction energy on the lattice vector c , and hence on the interlayer distance, is given in Figure 5. The equilibrium lattice vector c is found to be 6.76 Å, which corresponds to the interlayer distance of 3.38 Å. This value is slightly bigger than the experimental value of 3.35 Å (with lattice parameter 6.707 Å).³⁸

Unfortunately, no meaningful comparison with theoretical first-principles simulations is possible at present. Reasonable results of DFT–LDA computations, as performed by Telling and Heggge,³⁹ probably benefit from error compensation: the interaction around the van der Waals minimum is subject to a too-strong overbinding, whereas the long-range attractive interaction is not present. However, two different experimental approaches have been used to determine the interlayer cohesive energy of graphite. Already in 1956, Girifalco and Lad reported a value of 41 meV per atom ,⁴⁰ obtained by a heat of wetting experiment. In 1998, using nanotube collapse experiments, Benedict et al. determined a similar value of $35 \pm 10 \text{ meV/atom}$.⁴¹ The DC DFTB method gives a value of $38.5 \text{ meV atom}^{-1}$ for the cohesive energy, which is in excellent agreement with these experimental values.

We determined the lowest-energy stacking geometry by the dislocation glide of the graphene layers, one to each other, in the basal plane along two high-symmetry directions along the lattice vector a (denoted as X) and along the vector perpendicular to a , parallel to the layers (Y). We find two stacking-fault energies in X and one in Y with displacements that are the same as those reported in a DFT–LDA study³⁹ and that are in qualitative agreement with experiments.^{42,43} The relative stacking-fault energies in the basal plane can be found in Figure 6. The highest barrier is found at 6.7 meV/Å^2 in the X direction and at 2.8 meV/Å^2 in the Y direction. These values are $\sim 10\%$ smaller than those obtained

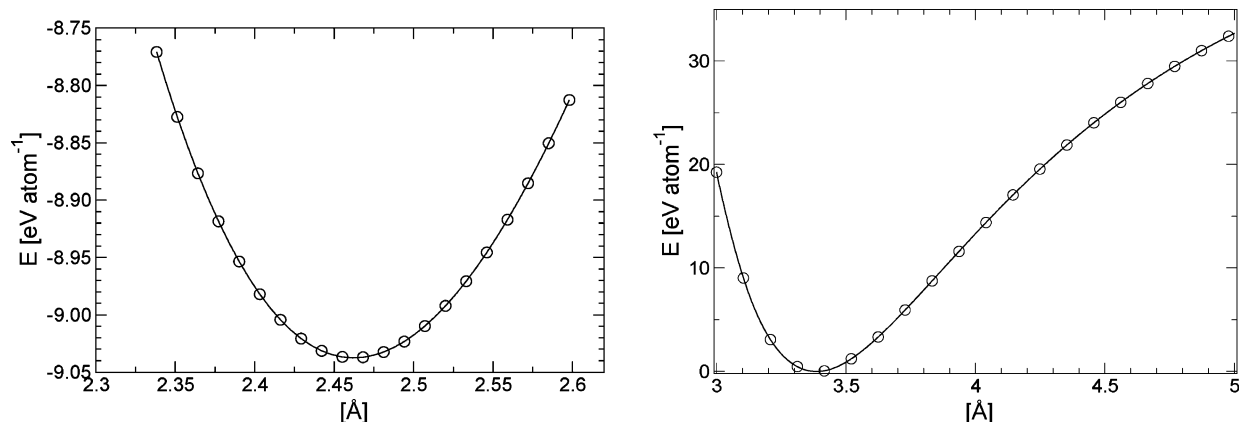


Figure 5. Dependence of the cohesion energy of graphite on the a (left) and $c/2$ (right) lattice parameters of the hexagonal unit cell. Equilibrium lattice parameters are $a = 2.465$ Å and $c/2 = 3.38$ Å ($c/2$ coincides with the interlayer distance).

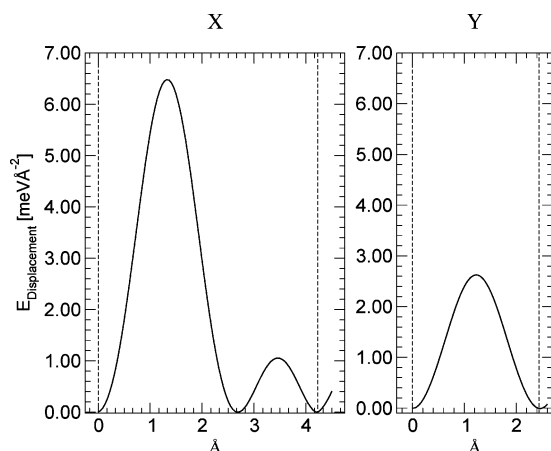


Figure 6. Intrinsic stacking-fault energy (in meV Å^{-2}) for relative layer displacement. Axis direction X denotes movement along the a lattice vector, and Y is the movement perpendicular to X parallel to the graphene planes. Unshifted hexagonal graphite is at 0.0 Å. The dashed lines on both sides of the graph indicate the periodicity for X and Y displacements.

by DFT–LDA calculations,³⁹ which probably reflects the LDA overbinding.

As the final test, we have calculated the isotropic bulk modulus for graphite. This quantity is defined as a second derivative of the energy with respect to the volume. It provides a very sensitive measure of the potential energy curvature close to the van der Waals minimum and, thus, is a good criterion for evaluating the accuracy of DFTB with dispersion correction applied to carbon nanostructures. Our calculated isotropic bulk modulus has been obtained from a volume change at 0 K with a constant c/a ratio (c and a are the lengths of the lattice vectors) and is found to be 330 GPa. This value almost matches the experimental value of 318 ± 11 GPa.^{44,45}

IV. Conclusions

The performance of ab initio, DFT, and DFTB methods for treating physisorption of H_2 on PAHs and on graphene was studied. Present LDA, GGA, and hybrid functionals are not adequate for the description of the long-range part of the dispersion interaction, whereas newer GGAs can describe short-range dispersion correctly. LDA overestimates the

short-range interaction; PBE-GGA is getting interaction energy and distances qualitatively correct, and B3LYP is even finding the interaction to be slightly repulsive. Only ab initio computations with a reasonable treatment of correlation and large basis sets provide a correct description of this interaction on the basis of a first-principle theory. However, if an a posteriori dispersion potential is added to the DFTB method, physisorption can be described adequately, whereas short-range interactions can still be treated quantum mechanically. Hence, the modified DFTB method allows simulations of processes where the topology of the atoms changes, including the influence of the dispersion interaction. This is particularly important for simulations of nanostructures, especially those including aromatic carbon systems as in fullerenes, nanotubes, and nano-onions.

Acknowledgment. We thank the Deutsche Forschungsgemeinschaft (DFG) and the joint PROBRAL action of DAAD (Germany)–CAPES (Brazil) for financial support. We thank Prof. Dr. Helio F. dos Santos and Nitesh Ranjan for helpful discussions and sharing their unpublished benchmark results. We also thank Dr. Annick Goursot and Dr. Christof Köhler for stimulating discussions.

References

- (1) London, F. Z. *Phys.* **1930**, *63*, 245.
- (2) Lein, M.; Dobson, J. F.; Gross, E. K. U. *J. Comput. Chem.* **1999**, *20*, 12–22.
- (3) Valdes, H.; Sordo, J. A. *J. Comput. Chem.* **2002**, *23*, 444–55.
- (4) Jensen, F. *Introduction to Computational Chemistry*; Odense University: Odense, Denmark, 1999.
- (5) Tran, F.; Weber, J.; Wesolowski, T. A.; Cheikh, F.; Ellinger, Y.; Pauzat, F. *J. Phys. Chem. B* **2002**, *106*, 8689–8696.
- (6) Dobson, J. F.; Das, M. P. *Topics in Condensed Matter Physics*; Nova: New York, 1994.
- (7) Grimme, S. *J. Comput. Chem.* **2004**, *25*, 1463–1473.
- (8) Chakarova, S. D.; Schröder, E. *J. Chem. Phys.* **2005**, *122*, 054102.
- (9) Cybulski, S. M.; Seversen, C. E. *J. Chem. Phys.* **2005**, *122*, 014117.

- (10) Xu, X.; Goddard, W. A. *J. Chem. Phys.* **2004**, *121*, 4068–4082.
- (11) Tao, J.; Perdew, P.; Staroverov, S.; Scuseria, G. *Phys. Rev. Lett.* **2003**, *91*, 416401.
- (12) Tao, J.; Perdew, P. *J. Chem. Phys.* **2005**, *122*, 114102.
- (13) Dion, M.; Rydberg, H.; Schröder, E.; Landgreth, D. C.; Lundqvist, B. I. *Phys. Rev. Lett.* **2004**, *92*, 246401.
- (14) von Lilienfeld, O. A.; Tavernelli, I.; Röthlisberger, U.; Sebastiani, D. *Phys. Rev. Lett.* **2004**, *93*, 153004.
- (15) Heine, T.; Zhechkov, L.; Seifert, G. *Phys. Chem. Chem. Phys.* **2004**, *6*, 980–984.
- (16) Hübner, O.; Gröss, A.; Fichtner, M.; Kloppe, W. *J. Phys. Chem. A* **2004**, *108*, 3019–3023.
- (17) Seifert, G.; Porezag, D.; Frauenheim, T. *Int. J. Quantum Chem.* **1996**, *58*, 185–192.
- (18) Porezag, D.; Frauenheim, T.; Köhler, T.; Seifert, G.; Kaschner, R. *Phys. Rev. B: Condens. Matter Mater. Phys.* **1995**, *51*, 12947–12957.
- (19) Elstner, M.; Porezag, D.; Jungnickel, G.; Elsner, J.; Haugk, M.; Frauenheim, T.; Suhai, S.; Seifert, G. *Phys. Rev. B: Condens. Matter Mater. Phys.* **1998**, *58*, 7260–7268.
- (20) Elstner, M.; Hobza, P.; Frauenheim, T.; Suhai, S.; Kaxiras, E. *J. Chem. Phys.* **2001**, *114*, 5149–5155.
- (21) Frauenheim, T.; Seifert, G.; Elstner, M.; Niehaus, T.; Köhler, C.; Amkreutz, M.; Sternberg, M.; Hajnal, Z.; Di Carlo, A.; Suhai, S. *J. Phys. C: Solid State Phys.* **2002**, *14*, 3015–3047.
- (22) Zhechkov, L.; Heine, T.; Seifert, G. *Int. J. Quantum Chem.* **2005**, in press.
- (23) Schönborn, F.; Schmitt, H.; Zimmermann, H.; Haeberlen, U.; Corminboeuf, C.; Grossmann, G.; Heine, T. *J. Magn. Reson.* **2005**, in press.
- (24) Rappé, A. K.; Casewit, C. J.; Colwell, K. S.; Goddard, W. A., III; Skiff, W. M. *J. Am. Chem. Soc.* **1992**, *114*, 10024–10035.
- (25) Köster, A. M.; Flores, R.; Geudtner, G.; Goursot, A.; Heine, T.; Patchkovskii, S.; Reveles, J. U.; Vela, A.; Salahub, D. R. *deMon*; NRC: Ottawa, Canada, 2003.
- (26) Boys, F. S.; Bernardi, F. *Mol. Phys.* **1970**, *19*, 553.
- (27) Frisch, M. J.; Trucks, G. W.; Schlegel, H. B.; Scuseria, G. E.; Robb, M. A.; Cheeseman, J. R.; Montgomery, J. A.; Vreven, T., Jr.; Kudin, K. N.; Burant, J. C.; Millam, J. M.; Iyengar, S. S.; Tomasi, J.; Barone, V.; Mennucci, B.; Cossi, M.; Scalmani, G.; Rega, N.; Petersson, G. A.; Nakatsuji, H.; Hada, M.; Ehara, M.; Toyota, K.; Fukuda, R.; Hasegawa, J.; Ishida, M.; Nakajima, T.; Honda, Y.; Kitao, O.; Nakai, H.; Klene, M.; Li, X.; Knox, J. E.; Hratchian, H. P.; Cross, J. B.; Adamo, C.; Jaramillo, J.; Gomperts, R.; Stratmann, R. E.; Yazyev, O.; Austin, A. J.; Cammi, R.; Pomelli, C.; Ochterski, J. W.; Ayala, P. Y.; Morokuma, K.; Voth, G. A.; Salvador, P.; Dannenberg, J. J.; Zakrzewski, V. G.; Dapprich, S.; Daniels, A. D.; Strain, M. C.; Farkas, O.; Malick, D. K.; Rabuck, A. D.; Raghavachari, K.; Foresman, J. B.; Ortiz, J. V.; Cui, Q.; Baboul, A. G.; Clifford, S.; Cioslowski, J.; Stefanov, B. B.; Liu, G.; Liashenko, A.; Piskorz, P.; Komaromi, I.; Martin, R. L.; Fox, D. J.; Keith, T.; Al-Laham, M. A.; Peng, C. Y.; Nanayakkara, A.; Challacombe, M.; Gill, P. M. W.; Johnson, B.; Chen, W.; Wong, M. W.; Gonzalez, C.; Pople, J. A. *Gaussian 03*, revision B.05; Gaussian, Inc.: Pittsburgh, PA, 2003.
- (28) Straatsma, T. P.; Aprà, E.; Windus, T. L.; Bylaska, E. J.; de Jong, W.; Hirata, S.; Valiev, M.; Hackler, M. T.; Pollack, L.; Harrison, R. J.; Dupuis, M.; Smith, D. M. A.; Nieplocha, J.; Tipparaju, V.; Krishnan, M.; Auer, A. A.; Brown, E.; Cisneros, G.; Fann, G. I.; Fruchtl, H.; Garza, J.; Hirao, K.; Kendall, R.; Nichols, J.; Tsemekhman, K.; Wolinski, K.; Anchell, J.; Bernholdt, D.; Borowski, P.; Clark, T.; Clerc, D.; Dachsel, H.; Deegan, M.; Dyall, K.; Elwood, D.; Glendening, E.; Gutowski, M.; Hess, A.; Jaffe, J.; Johnson, B.; Ju, J.; Kobayashi, R.; Kutteh, R.; Lin, Z.; Littlefield, R.; Long, X.; Meng, B.; Nakajima, T.; Niu, S.; Rosing, M.; Sandrone, G.; Stave, M.; Taylor, H.; Thomas, G.; van Lenthe, J.; Wong, A.; Zhang, Z. *NWChem, A Computational Chemistry Package for Parallel Computers*, version 4.6; Pacific Northwest National Laboratory: Richland, WA, 2004.
- (29) Kendall, R. A.; Dunning, T. H.; Harrison, R. J. *J. Chem. Phys.* **1992**, *96*, 6769–6806.
- (30) Godbout, N.; Salahub, D. R.; Andzelm, J.; Wimmer, E. *Can. J. Chem.* **1992**, *70*, 560–571.
- (31) Dunning, T. H. *J. Chem. Phys.* **1989**, *90*, 1007–1023.
- (32) Vosko, S. H.; Wilk, L.; Nusair, M. *Can. J. Phys.* **1980**, *58*, 1200–1211.
- (33) Perdew, J. P.; Burke, K.; Ernzerhof, M. *Phys. Rev. Lett.* **1996**, *77*, 3865–3868.
- (34) Becke, A. D. *J. Chem. Phys.* **1993**, *98*, 5648–5652.
- (35) Lee, C.; Yang, W.; Parr, R. G. *Phys. Rev. B: Condens. Matter Mater. Phys.* **1988**, *37*, 785–789.
- (36) Albertazzi, E.; Domene, C.; Fowler, P. W.; Heine, T.; Seifert, G.; Van Alsenoy, C.; Zerbetto, F. *Phys. Chem. Chem. Phys.* **1999**, *1*, 2913–2918.
- (37) Porezag, D.; Jungnickel, G.; Frauenheim, T.; Seifert, G.; Ayuela, A.; Pederson, M. R. *Appl. Phys. A* **1997**, *64*, 321–326.
- (38) Zhao, Y. X.; Spain, I. L. *Phys. Rev. B: Condens. Matter Mater. Phys.* **1989**, *40*, 993997.
- (39) Telling, R. B.; Heggie, M. I. *Philos. Mag. Lett.* **2003**, *83*, 411–421.
- (40) Girifalco, L. A.; Lad, R. A. *J. Chem. Phys.* **1956**, *25*, 693–697.
- (41) Benedict, L. X.; Chopra, N. G.; Cohen, M. L.; Zettl, A.; Louie, S. G.; Crespi, V. H. *Chem. Phys. Lett.* **1998**, *286*, 490–496.
- (42) Snyder, S. R.; Gerberich, W. W.; White, H. S. *Phys. Rev. B: Condens. Matter Mater. Phys.* **1993**, *47*, 10823–10831.
- (43) Ouseph, P. J. *Phys. Rev. B: Condens. Matter Mater. Phys.* **1996**, *53*, 9610–9613.
- (44) Gauster, W. B.; Fritz, I. J. *J. Appl. Phys.* **1974**, *45*, 3309–3314.
- (45) Jansen, H. J. F.; Freeman, A. J. *Phys. Rev. B: Condens. Matter Mater. Phys.* **1987**, *35*, 8207–8214.